CIRP Annals - Manufacturing Technology 57 (2008) 89–92

Contents lists available at ScienceDirect

CIRP Annals - Manufacturing Technology

journal homepage: http://ees.elsevier.com/cirp/default.asp

Surface finishes from turning and facing with round nosed tools

T.H.C. Childs (1)[a,*], K. Sekiya [b], R. Tezuka [b], Y. Yamane [b], D. Dornfeld (1)[c], D.-E. Lee [c], S. Min [c], P.K. Wright [c]

[a] School of Mechanical Engineering, University of Leeds, Woodhouse Lane, Leeds, UK
[b] Graduate School of Hiroshima University, Higashi-Hiroshima, Japan
[c] College of Engineering, University of California, Berkeley, USA

ARTICLE INFO

Keywords:
Precision
Machining
Surface roughness

ABSTRACT

The range of surface roughnesses, and particularly the minimum roughnesses, achievable mainly with cemented carbide but also with single crystal diamond round nosed turning and facing inserts, has been experimentally studied, machining aluminium on engineering and precision lathes. Insert edge sharpness and roughness measurements and characteristic variations with feed rate of machined surface profile are presented. When machine tool limits are avoided, R_z values down to 0.02 times the insert edge radii have been obtained.

1. Introduction

It is well-known, in turning or facing at a feed f with a tool of nose radius r_n, that the peak-to-valley roughness that is created, R_z for example, usually equals or exceeds the kinematic value $f^2/(8r_n)$ and that, below some limiting value of f, R_z becomes independent of f and may even increase as f reduces further. Fig. 1 presents results of previous studies [1–11] on ferrous and non-ferrous work materials, for single crystal diamond (SCD), ceramic (PCD and PCBN) and cemented carbide tools. Given reasons for roughnesses larger than kinematic include machine tool limits (dynamic stiffness, feed control and bearing clearance effects), work material (it is responsible for process forces and how the chip separates from the work) and the insert edge quality (roughness along the edge and radius in the plane normal to the edge).

However, only three of [1–11] record cutting edge radius values and none investigates roughness along the edge. Further, some record R_a, some R_z and some present surface profile charts. Assumptions have been made here to create the unified (Fig. 1). Nonetheless, given typical insert edge radii for cemented carbides of 10–20 μm and for SCD of maybe 0.1 μm, Fig. 1's minimum peak-to-valley heights of 2–8 μm (cemented carbides) and 0.02–0.08 μm (SCD) suggest perhaps that these might be proportional to edge radius, with the constant of proportionality in the range 0–0.5.

The present paper reports new data from turning and facing aluminium with SCD and cemented carbide tools, on precision and general engineering machine tools, at feeds from 2 to 670 μm/rev, that suggest that in Fig. 1 minimum roughnesses are in fact machine tool limits.

There is a minimum R_z proportional to edge radius but the constant of proportionality is ≈0.02 (at least for aluminium as a work material). As-manufactured carbide insert edge roughness rarely limits work material surface finish.

2. Experiments

1000 series aluminium was turned and faced in two different laboratories on complementary machine tools, using the same insert grades at both sites. A summary is in Table 1. At Hiroshima, 100 mm diameter Al 1075 bar (HV 210 MPa) was turned on a mechanically controlled engine lathe (10.2 kW Okuma, MT1 in Table 1) regarded as having a high precision for its class. 60 mm diameter discs from the bar were faced on a precision diamond turning machine (Toshiba Machine Co. ULC-100A, MT2). At Berkeley, 60 mm diameter discs cut from Al 1100 cold rolled plate (HV 420 MPa) were faced on a precision diamond turning machine (Rank Pneumo MSE-326, MT3) better protected against damage from overload than was the ULC machine. Cemented carbide and SCD insert tools were used. HTi10 (uncoated), UP20M (TiN coated) and UC5105 (Al_2O_3 on TiCN coated) carbides were from Mitsubishi Carbide. T725X was from Toshiba Tungaloy. The SCD tools 1 and 2 were supplied by Sumitomo Electric Industries Ltd. SCD1 addressed the work with zero side and back rake angle. SCD2 was cut to present a large negative back rake to the work. It was claimed to be sharper than SCD1. The cemented carbide tools were used with side rakes of +5° (TP inserts) or −6° (CN inserts) at Hiroshima and +6° side rake at Berkeley.

With MT1, 20 mm lengths of bar were turned at feeds from 670 to 290 (depending on r_n) to 25 μm/rev. Then turning was always confined to the inserts' nose radius regions. Cutting speed 200 m/min, depth of cut a_p 0.5 mm and no cutting fluid were used, after preliminary tests (speed 100–200 m/min; a_p 0.2, 0.5 mm; oil mist, dry) found negligible dependence of surface finish on these. Inserts were checked for tool wear by low-power microscope. If none was observed, the same corner continued to be used. If wear was observed, a decision was made whether to change the corner or not.

* Corresponding author.

0007-8506/$ – see front matter © 2008 CIRP.
doi:10.1016/j.cirp.2008.03.121

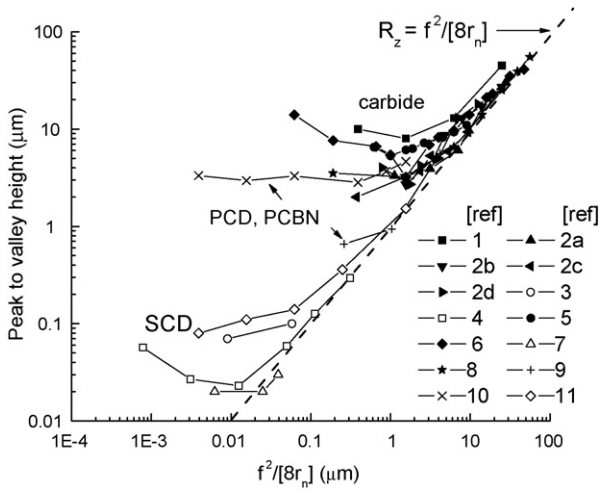

Fig. 1. Surface roughness variation with feed and tool nose radius, from [1–11]; refs. 2a–d refers to different r_n.

With MT2 and MT3, 5–6 mm width annuli were faced at feeds of 15, 10, 5, 2 (MT2) and 25, 10, 5 (MT3) μm/rev, adjusting spindle speeds to keep cutting speed in the range 200–100 m/min. a_p was varied between 5 and 2 μm, needed to limit cutting forces. Cutting fluid was used (oil mist MT2, methanol drip MT3), to aid swarf removal. Disc truing and subsequent tests over the range of feeds were carried out with a single insert corner, with a microscopic check for wear being made at the end.

The nose radius region edge radii r_e of the cemented carbide inserts were obtained by stylus profilometry. Inserts were held symmetrically in place beneath the stylus, with a corner to be measured at the highest point. The stylus was traversed perpendicular to the cutting edge, from the rake face to the relief face. A best circle was fitted to the raw data profiles. The edge radii of the SCD inserts were too small to be measured in this way.

Cutting edge roughness was also measured for the carbide inserts, traversing the stylus across the tool nose relief face, parallel to the cutting edge and as close to the edge as could be judged. The data was used in two ways. Firstly, it was used graphically to construct the expected kinematic roughness of machined surfaces, taking the roughness imperfection of the tool nose into account. Secondly, the nose radius form was removed from the data, followed by Gaussian filtering (upper cut-offs 250, 80, 25, 8 and 2.5 μm). R_z values that were then extracted were also used as estimates of the expected machined surface kinematic peak-to-valley heights.

Workpiece roughness parameters were measured. R_z (10 point height) is reported here. Chart recordings were also made of the profiles. Different profilometers (stylus type unless otherwise described) were used for the tests on the MT1/2/3 machines, because of the machines' different locations. For MT1, a Kosaka Surfcorder SE-30D was used, with its cutoff set at "$R + W$". For MT2, a Tokyo Seimitsu Accretech 3000A was used, with cut-off 0.25 mm. For MT3, a RTH Form Talysurf 120L and a white light interferometer (Wyko NT3300S) were used, both with cut-offs 0.25 mm. Comparisons were made between profilometers. Between-machine measurement differences were similar to within-machine scatter except in one case (see later).

Table 1
Work, machine tool and insert combinations

Work, machines		Insert description	r_e (μm)
Al 1075	Al 1100		
MT1/2	MT3	HTi10 TPGN1603xx[a]	6 ± 2
MT1	MT3	UP20M[b] TPMN160308	55 ± 5
MT1	MT3	UC5105[c] TPMN160304	60 ± 5
MT1	–	T725X[c] CNMG120408	80 ± 5
MT2	–	SCD1 r_n 0.5 mm	$<0.1_{nom}$
MT2	–	SCD2 r_n 0.5 mm	$<0.1_{nom}$

[a] xx = 0.4, 0.8, 1.6 mm.
[b] PVD coated.
[c] CVD coated.

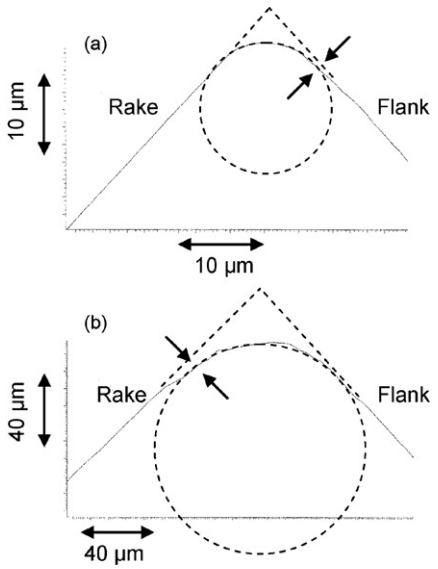

Fig. 2. Tool nose region cutting edge profiles (a) HTi10 160316 and (b) UC5105 inserts.

3. Results

Fig. 2 shows typical edge sharpness observations. In neither is the edge simply a circular blend from the rake to the flank. The opposed arrows show that the edge circle is inset in (a) from the flank and (b) from the rake face. In (b) the edge is closer to three segments than a circle. The edge radii in Table 1 are ranges from at least six corners.

The values for the SCD inserts are upper bounds from manufacturer's estimates.

The top left corner of Fig. 3 shows, as an example, the cutting edge roughness round the tool nose of a UC5105 insert, scaled to the typical proportions at which work surface roughness traces are displayed. The remaining parts are kinematic roughnesses derived from this, by repeatedly indexing the insert profile 0.1, 0.05 and 0.025 mm, to create estimated work surface profiles from feeds as marked. Fig. 4 plots R_z for all the work surface roughnesses derived in this way (from visual inspection of peak-to-valley heights). It also shows the alternative estimates of R_z from Gaussian filtered insert roughness profiles. There is a reasonable agreement between the two methods. For the carbide inserts, the influence of edge roughness on R_z may be expected to exceed that of nose radius as feeds reduce below 0.05 mm/rev.

Fig. 5 shows R_z after turning Al 1075 on MT1. No tool wear was seen during these tests, except from T725X at feeds less than 0.1 mm/rev. Then the relief face coating delaminated. For this insert there are two sets of data, unworn and worn (VB_{max} up to

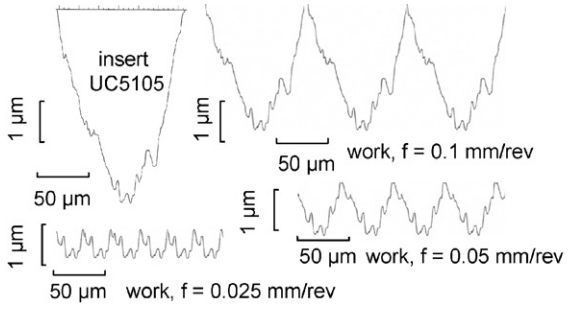

Fig. 3. UC5105 cutting edge roughness and work surface kinematic profiles derived from it.

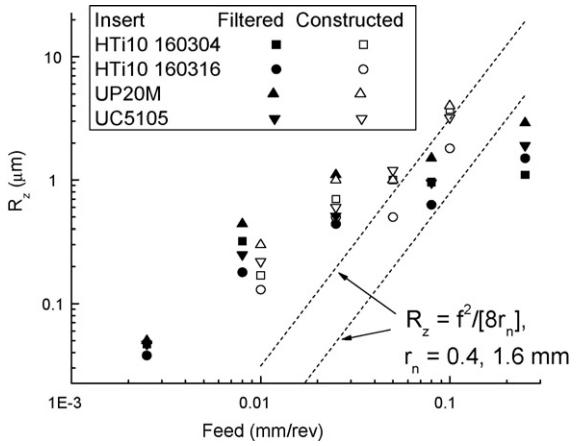

Fig. 4. Kinematic roughness constructed and filtered from insert profiles, compared to $f^2/[8r_n]$.

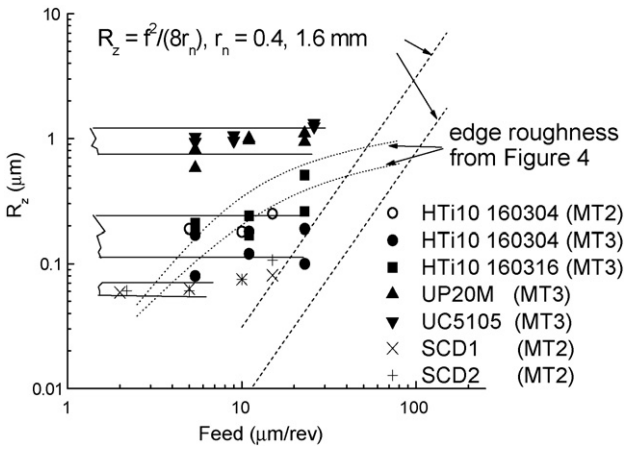

Fig. 6. Dependence of R_z on feed, MT2/3 tests.

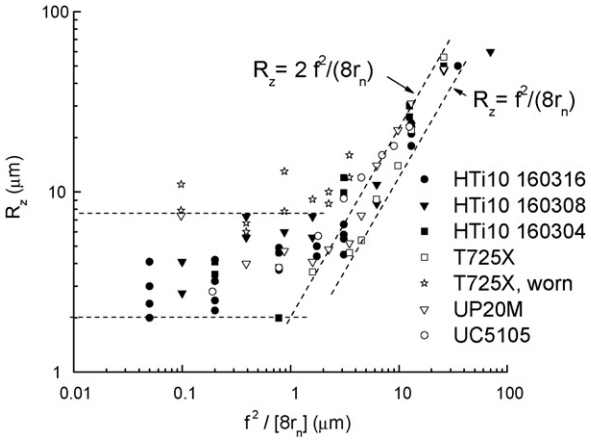

Fig. 5. Dependence of R_z on $f^2/[8r_n]$, MT1 tests.

0.26 mm). Because of its wear, T725X was not used for the MT2 and MT3 tests. Fig. 5 shows that at large feeds, R_z was from 1 to 2 times the kinematic roughness $f^2/[8r_n]$. At low feeds, R_z was independent of feed, with values from 2 to 8 μm (in the absence of insert wear), the same for all inserts.

Fig. 6 collects R_z from the MT2 and MT3 tests. SCD1 and 2 gave an optically good mirror finish at feeds of 10 μm/rev and less, with R_z down to 60 nm. R_z from Al 1075 faced by HTi10 160304 on MT2 was of the same size as from Al 1100 faced by HiTi10 160304 and 160316 on MT3, namely ≈ 0.2 μm, except that measurements from the 160304 insert used on MT3 obtained by white light interferometry, were ≈0.1 μm. Apart from this, the data from HTi10 inserts establish an equivalence between facing Al 1075 on MT2 and Al 1100 on MT3. In all cases the finish was visually of borderline mirror quality. Facing with UP20M and UC5105 on MT3 gave R_z from 0.8 to 1.1 μm, both independent of feed and partially reflective, with fine circumferential scoring.

Fig. 7 shows work surface profiles at different feeds.

Parts a and b, for which $f^2/[8r_n] = 7$ and 0.4 μm, represent conditions (Fig. 5) in which R_z (a) follows the kinematic trend and (b) is independent of feed. In (a) feed marks are seen to be deformed from their kinematic shape on their trailing faces, with height h 1.7 times the kinematic value; the observed R_z of up to twice the kinematic value (Fig. 5) is compatible with this. In (b) the waveform has a repeat distance twice the feed. Machine tool vibration would cause this. Parts (c)–(e) are from precision machining and (c) has a periodicity of 15 μm, equal to the feed, and a wave form that might be expected from edge roughness (after the manner of Fig. 3). By the stage feed has reduced to 5 μm (part d), a less regular wave-form is generated. For this surface, stylus profilometry gave $R_z = 0.17$ μm; observation of peak-to-valley heights over the 90 μm trace length of part d gives R_z closer to 0.1 μm. This is similar to the differences in R_z from stylus and white light machines. Finally part (e) is from facing with a SCD insert. $f^2/[8r_n] = 6$ nm. Such a roughness is seen superimposed on an approximately square wave, amplitude 20 nm, wavelength 50 μm. As machine RPM was changed to maintain cutting speed constant, this wavelength remained unchanged. It is thus believed to arise from a MT2 feed drive imperfection.

4. Discussion

R_z reducing with feed, then becoming independent of it at $f^2/[8r_n] \approx 2$–8 μm (Fig. 5), when machining with carbide inserts on an engineering lathe, is the same as in Fig. 1. That the transition and attainable roughnesses do not depend on insert edge radius points to their being determined by machine tool precision limits. A lower machine tool limit from the present work ($R_z \approx 60$ nm) comes from facing with SCD inserts on a precision lathe.

New results from this work come from facing with carbide inserts on precision lathes. Then (Fig. 6) minimum R_z values have been independent of feed and dependent on edge radius. Comparing the R_z values for HTi10, UP20M and UC5105 inserts with edge radii in Table 1, minimum R_z values are 0.02 ± 0.01 times the edge radii.

Carbide insert edge roughness (Figs. 3 and 4) could be expected to determine surface finish over limited feed ranges (from 0.1 mm/rev, Fig. 4, down to feeds at which edge radius determines roughness). But in the present work (with HTi10 inserts) R_z less than that expected from edge roughness has been measured (for UP20M and UC5105 inserts, edge radius has caused poorer finish than edge roughness). How that arises is an open question. In Fig. 4, the derived R_z values are proportional to $f^{1/2}$: this is as expected for a random rough surface [12] and reinforces the validity of methods to create the figure. The different R_z values from stylus and white light profilometry, for surfaces faced by the HTi10 160304 inserts, introduce an uncertainty into the true value, but even the upper estimate of ≈ 0.2 μm is less, at the feeds 25 and 10 μm/rev, than expected from Fig. 4. Maybe the insert edge becomes effectively smoothed by filling of its roughness valleys with work material.

From this paper's results, R_z caused by edge radius exceeds that caused by nose radius (feed marks) once $f^2/[8r_n] < (0.02 \pm 0.01)r_e$, or $f^2/[r_n r_e] < 0.16 \pm 0.08$. As f^2/r_n is the uncut chip thickness at the part of the cutting edge where the feed mark peaks are created [4], the inequality suggests a critical uncut chip thickness to cutting edge radius ratio at the finished surface, ≈0.15, below which edge sharpness determines finish. 0.15 is within the range of critical uncut chip thickness to cutting edge radius ratio for transitions from cutting to ploughing in precision orthogonal cutting studies [13–16]. The relationship between the present work's secondary cutting edge results and this other orthogonal cutting literature is developed in a companion paper [17].

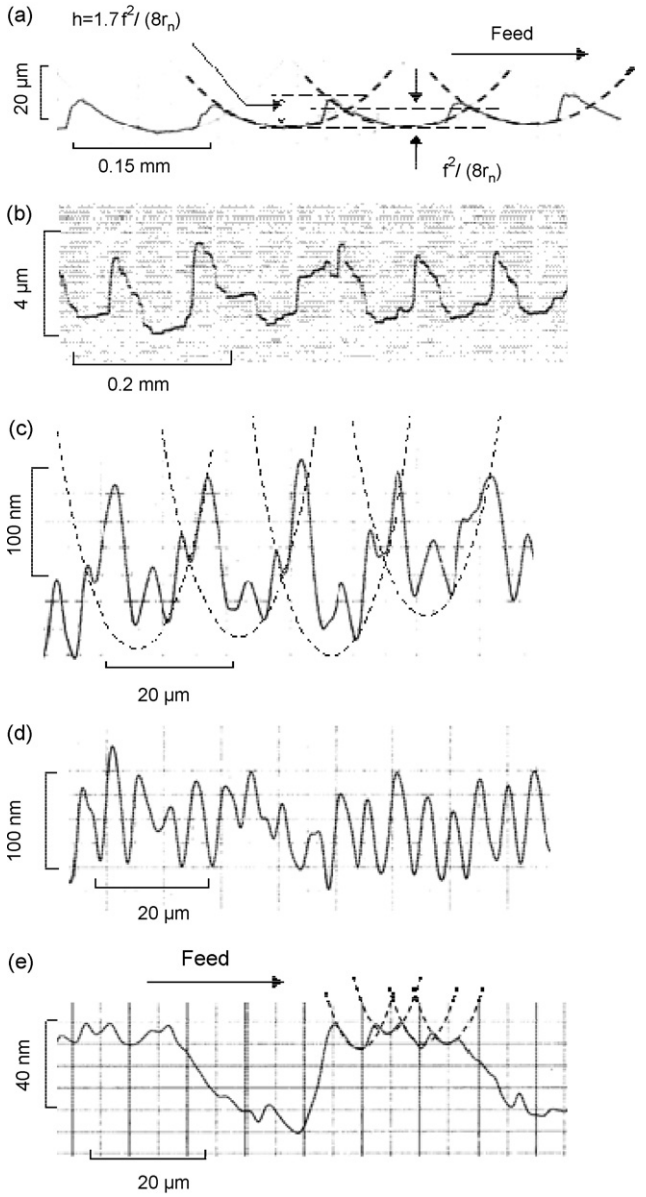

Fig. 7. Representative work surface profiles: (a) HTi10 160304, Al1075, MT1, $f = 150$ µm/rev; (b) HTi10 160308, Al1075, MT1, $f = 50$ µm/rev; (c) HTi10 160304, Al1075, MT2, $f = 15$ µm/rev; (d) HTi10 160304, Al1075, MT2, $f = 5$ µm/rev; (e) SCD1, Al1075, MT2, $f = 5$ µm/rev.

5. Conclusion

As feed is reduced in turning or facing with round nosed cemented carbide inserts, the insert feature that controls surface roughness changes from nose radius to edge sharpness. An expected dependence on edge roughness has not been observed. At the lowest feeds, R_z becomes independent of feed and proportional to edge radius, unless a machine tool precision limit intervenes. For aluminium work materials, the constant of proportionality is 0.02 ± 0.01. This value leads to surface finish controlled by edge sharpness when $f^2/[r_n r_e] < 0.16 \pm 0.08$.

Acknowledgments

This work was supported by funding for visiting positions for one of us (THCC) from the Venture Business Laboratory of Hiroshima University and the Springer endowment of the University of California at Berkeley.

References

[1] Shaw MC, Crowell JA (1965) Finish Machining. *Annals of the CIRP* 13:5–22.
[2] Petropoulos PG (1973) The Effect of Feed Rate and of Tool Nose Radius on the Roughness of Oblique Finish Turned Surfaces. *Wear* 23:299–310.
[3] Sugano T, Takeuchi K, Goto T, Yoshida Y (1987) Diamond Turning of an Aluminium Alloy for a Mirror. *Annals of the CIRP* 36(1):17–20.
[4] Moriwaki T, Okuda K (1989) Machinability of Copper in Ultra-Precision Micro-Diamond Cutting. *Annals of the CIRP* 38(1):115–118.
[5] Grzesik W (1996) A Revised Model for Predicting Surface Roughness in Turning. *Wear* 194:143–148.
[6] Petropoulos G, Karahaliou H (1999) Investigating into the Effect of Small Feed Rate Values on the Roughness Produced by Turning Operations. *Proceedings of the 3rd BALKANTRIB International Conference*, Sinaia, Roumania, Vol. 1, 139–146.
[7] Cheung CF, Lee WB (2001) Characteristics of Nano-Surface Generation in Single Point Diamond Turning. *International Journal of Machine Tools & Manufacture* 41:851–875.
[8] Petropoulos GP, Torrance AA, Pandazosas CN (2003) Abbott Curve Characteristics of Turned Surfaces. *International Journal of Machine Tools & Manufacture* 43:237–243.
[9] Ozel T, Hsu T-K, Zeren E (2005) Effects of Cutting Edge Geometry, Workpiece Hardness, Feed Rate and Cutting Speed on Surface Roughness and Forces in Finish Turning of Hardened AISI H13 Steel. *International Journal of Advanced Manufacturing Technology* 25:262–269.
[10] Liu K, Melkote SN (2006) Effect of Plastic Side Flow on Surface Roughness in Micro-Turning Process. *International Journal of Machine Tools & Manufacture* 46:1778–1785.
[11] Okuda K, Ogawa E (2006) Study on Step at Grain Boundary in Ultra-Precision Cutting of Phosphor Bronze. *Proceedings of the 8th ICTMP*, JSPE, Japan, 393–396.
[12] Thomas TR (1982) *Rough Surfaces*. Longman Group, New York . pp. 116–117.
[13] Taminiau DA, Dautzenberg JH (1991) Bluntness of the Tool and Process Forces in High-Precision Cutting. *Annals of the CIRP* 40(1):65–68.
[14] Lucca DA, Seo YW (1994) Aspects of Surface Generation in Orthogonal Ultraprecision Cutting. *Annals of the CIRP* 43(1):43–46.
[15] Yuan ZJ, Zhou M, Dong S (1996) Effect of Diamond Sharpness on Minimum Cutting Thickness and Cutting Surface Integrity in Ultraprecision Cutting. *Journal of Materials Processing Technology* 62:327–330.
[16] Liu X, DeVor RE, Kapoor SG (2006) An Analytical Model for the Prediction of Minimum Chip Thickness in Micromachining. *Transaction of the ASME Journal of Manufacturing Science and Engineering* 128:474–481.
[17] Childs THC, Dornfeld D, Lee D-E, Min S (in press) (2008) The Influence of Cutting Edge Sharpness on Surface Finish in Facing with Round Nosed Tools. In: *Proceedings of the 3rd CIRP International Conference on High Performance Cutting*, Dublin, Ireland.